Available online at www.sciencedirect.com

SCIENCE DIRECT®

Journal of Molecular Catalysis A: Chemical 246 (2006) 140–145

JOURNAL OF MOLECULAR CATALYSIS A: CHEMICAL

www.elsevier.com/locate/molcata

Deactivation of $Ni/K_2O-La_2O_3-SiO_2$ catalyst in hydrogenation of *m*-dinitrobenzene to *m*-phenylenediamine

Lei Zhao, Jixiang Chen*, Jiyan Zhang

Department of Catalytic Science and Engineering, School of Chemical Engineering and Technology,
Tianjin University, Tianjin 300072, PR China

Received 26 August 2005; received in revised form 1 November 2005; accepted 1 November 2005

Abstract

A novel supported nickel-based catalyst, $Ni/K_2O-La_2O_3-SiO_2$, was prepared and its catalytic stability and deactivation in the catalytic hydrogenation of *m*-dinitrobenzene to *m*-phenylenediamine were investigated. With ethanol as solvent, under the reaction conditions of 373 K, 3.0 MPa, catalyst/*m*-dinitrobenzene mass ratio of 3% and solvent/*m*-dinitrobenzene mass ratio of 2, the conversion of *m*-dinitrobenzene and the selectivity of *m*-phenylenediamine were 99.9% and over 99.6%, respectively. There was a trend of catalyst deactivation during recycles and the catalysts before and after reaction were characterized by means of N_2 adsorption–desorption, X-ray diffraction (XRD), thermogravimetric analysis (TGA)/differential thermal analysis (DTA), scanning electron microscopy (SEM) and atomic absorption spectrometry (AAS). The results indicated that the catalyst deactivation could be mainly ascribed to the surface coverage and the pore blockage with bulky molecular species. Additionally, the loss of active component nickel could also result in the catalyst deactivation to some extent.

Keywords: Catalytic hydrogenation; *m*-Phenylenediamine; *m*-Dinitrobenzene; Deactivation

---

1. Introduction

m-Phenylenediamine (MPD) is an important organic intermediate for the synthesis of some polymers, dyestuff and other materials. With the increasing application of engineering materials (especially aromatic polyamide fiber and polyurethane), the demand of MPD is growing. Various methods have been used to synthesize MPD from *m*-dinitrobenzene (MDNB), such as iron–acid reduction (the traditional process), electrolytic reduction and catalytic hydrogenation. The major disadvantage of the iron–acid reduction process is the generation of a large amount of ferric oxide sludge, which raises severe disposal problems and is therefore strictly restricted in many countries, while the electrolytic reduction method is so power-consuming that it is not economic. Alternatively, the catalytic hydrogenation of MDNB in liquid phase is an attractive technology for its advantages, such as high product yield, mild reaction conditions, less pollution to environment and so on [1]. Supported noble metals such as Pd/C [2,3] and Raney nickel [4] are the commonly used catalysts for the hydrogenation of MDNB. However, the rather rare resource and high price of noble metals restrict their application. As to Raney nickel, there exist some drawbacks in the industrial process, such as the severe corrosion and the pollution resulted from its preparation process and the safety problem during its storage and application. Supported nickel catalysts have been widely used in many hydrogenation reactions [5–10] due to their high reactivity, easy availability and low price. Unfortunately, few works about hydrogenation of MDNB over supported nickel catalysts have been reported so far.

Recently, our group studied the preparation and the catalytic performance of the supported nickel catalysts for the hydrogenation of MDNB and found that the silica supported catalysts showed better catalytic performance than Raney nickel, especially when they were modified with some rare earth metal oxides or/and alkali metal oxides [11–13]. These promoters not only increased the dispersivity of nickel species, but also modified the surface properties of the catalysts (e.g., basicity), all of which were in favor of improving the catalyst reactivity remarkably. In the present work, the stability and the deactivation of $Ni/La_2O_3-K_2O-SiO_2$ (labeled as NLKS) catalyst were investigated systematically.

---

* Corresponding author. Tel.: +86 22 27890865; fax: +86 22 27890865.
E-mail address: jxchen@tju.edu.cn (J. Chen).

1381-1169/$ – see front matter © 2005 Elsevier B.V. All rights reserved.
doi:10.1016/j.molcata.2005.11.003

2. Experiment

2.1. Catalyst preparation

Ni/La_2O_3-K_2O-SiO_2 catalyst was prepared by conventional incipient impregnation method. The support, a commercial silica manufactured by Tianjin Research and Design Institute of Chemical Industry, was impregnated with an aqueous solution containing $Ni(NO_3)_2$, $La(NO_3)_3$ and KNO_3, and then placed at room temperature for 12 h. After drying at 383 K for 8 h and air calcination at 773 K for 4 h, the catalyst sample was reduced at 723 K for 2 h in a flowing hydrogen–argon mixture with a volume ratio of 1:9 and the fresh catalyst was obtained. The catalyst after reduction was transferred into the vessel containing ethanol under the protection of flowing hydrogen–argon mixture, i.e., it was always handled under an air-free condition.

2.2. Activity test

The liquid phase hydrogenation of MDNB was carried out in a 250 mL stainless steel autoclave reactor, which was charged with MDNB (40 g) and fresh NLKS catalyst (1.2 g) in ethanol (100 mL, as solvent). At first, air was flushed out of the reactor with nitrogen at room temperature and then hydrogen was fed into the reactor. After replacing nitrogen with hydrogen, the reactor was heated to 373 K and charged with hydrogen to 3.0 MPa, and then the hydrogenation reaction started with stirring at 1000 rpm. During the catalytic run, samples were withdrawn periodically and analyzed with a gas chromatograph equipped with a flame ionization detector (FID) and an OV-101 capillary column.

2.3. Catalyst characterization

X-ray diffraction (XRD) patterns were obtained with a RIGAKU D/MAX-2500 diffractometer with Cu Kα radiation (40 kV, 100 mA). The average nickel crystallite size was estimated from XRD line-broadening by employing Scherrer equation. Thermogravimetric analysis (TGA) and differential thermal analysis (DTA) were carried out with a Pyris Diamond TG/DTA instrument in an air flowing of 150 mL/min at a heating rate of 15 K/min. BET specific surface area and pore size distribution were measured with a SORPTOMATIC 1900 surface analysis apparatus by N_2 volumetric adsorption method at 77 K. The surface morphology and the local composition of the catalyst were obtained by scanning electron microscopy (SEM) on a PHILIPS XL-30 ESEM equipped with an energy dispersive X-ray emission analyzer (EDX). The Ni loadings of the catalysts were determined by AAS on a HITACHI 180-80 Polarized Zeeman Atomic Absorption Spectrophotometer.

3. Results and discussion

3.1. Catalyst stability

Table 1
Stability result of catalyst for catalytic hydrogenation of MDNB

Recycle times	Reaction time (min)	Conversion of MDNB (%)	Selectivity of MPD (%)
1	370	99.9	99.6
6	408	99.9	99.7
11	443	99.9	99.7
16	470	99.9	99.6
19	500	99.9	99.6
20	550	99.9	99.7
21	720	99.9	99.7

Table 1 shows the results of the catalyst stability tests in the hydrogenation of MDNB. In the test, a few of the catalyst were lost when the product was drawn out of the reactor and the separation of product and the catalyst and so a spot of the fresh catalyst (about 10 wt.% of the initial catalyst amount) corresponding to the loss was added before next run (apart from the last two recycles). In the whole experimental process, the catalyst was always stored carefully in ethanol in order to avoid its oxidation by air. In the first 19 recycles, the conversion of MDNB reached 99.9% and the selectivity of MPD was over 99.6% in 370–500 min. While in the last two recycles, it took a longer time to reach the similar MDNB conversion and MPD selectivity as the first 19 recycles, partly due to no fresh catalyst added. Whether or no, there was a trend that the reaction time became longer in order to reach 99.9% of MDNB conversion along with the recycles, which indicated that there really existed the catalyst deactivation.

3.2. Catalyst deactivation analysis

The activity of NLKS catalyst decreased along with the recycles and the investigation on the catalyst deactivation was carried out. In the following experiments, the fresh NLKS catalyst was obtained from the reduction of the catalyst precursor at 723 K in a flowing hydrogen–argon mixture with a volume ratio of 1:9 for 2 h, and the used one was the one recycled for 21 times.

3.2.1. XRD results

Sintering of metal particles resulting in loss of active surface area is an irreversible reason for catalyst deactivation and sintering can be easily followed by XRD particle size measurements [14]. The XRD patterns of the fresh NLKS catalyst and the used one are presented in Fig. 1 and they show the similar diffraction patterns. A broad peak around $2\theta = 22°$ was assigned to the silica gel phase, which was a typical amorphous structure. The peaks around $2\theta = 44.4°$, $51.8°$ and $76.4°$ were ascribed to metallic nickel and the peaks around $2\theta = 37.2°$, $43.2°$ and $62.9°$ to nickel oxide, which indicated that the catalyst was not reduced entirely in the activation phase. Because the Ni^0 was the active site for the hydrogenation, the size of nickel crystallites might be corresponding to the active areas. As shown in Table 2, the average size of the nickel crystallites on the used sample was 15.9 nm, which was only a 0.2 nm larger than that on the fresh one.

For supported metal catalysts, sintering due to temperature driven migration and coalescence of metal particles on supports is generally unlikely because most liquid phase reactions are

Table 2
Properties of fresh catalyst and used catalyst

Catalyst	Ni content (wt.%)[a]	Specific surface areas (m^2/g)	Specific pore volume (cm^3/g)	Average pore radius (nm)	Nickel crystallite size (nm)[b]
Fresh	22.7	139.9	0.643	9.192	15.7
Used	20.3	125.6	0.461	7.341	15.9

[a] Data obtained from AAS measurement.
[b] Calculated with Scherrer formula using (2 0 0) reflection of fcc Ni.

carried out at comparatively low temperatures [15]. Xiao and Hofmann [16] studied the deactivation of $Ni/SiO_2/Al_2O_3$ catalyst in the hydrogenation of 3-hydroxypropanal (HPA) and found that sintering was not a main reason because the reaction temperature was less than 353 K. They considered that sintering normally started only at temperature above 473 K. However, the sintering of supported catalysts also occured even at room temperature. For example, Schuurman et al. [17] found that, in the oxidation reaction of methyl-α-D-glucoside at 323 K on Pt/C catalyst, platinum particle size increased from 2.2 to 3.2 nm after one batch experiment, and to 8.0 nm after 25 batch experiments. They considered the growth of the Pt particles was due to the dissolution and subsequent redepsition of platinum, for the platinum ions were found in the solution during oxidation. Bett et al. [18] had the similar opinion. Thus, whether the sintering of supported metal catalysts occurs is related to the properties of the catalysts and the reaction conditions concerned.

In the present work, the liquid-phase hydrogenation reaction was carried out at 373 K, which was much lower than the Hütting temperature (about 518 K) and the Tamman temperature (about 863 K) of nickel. Meanwhile, the growth of the nickel crystallites was not remarkable as above-mentioned, thus, the deactivation of the present catalyst did not result from the sintering of the nickel crystallites essentially.

3.2.2. *TGA and DTA results*

Fig. 2 depicts the TG curves of the fresh catalyst and the used one. In the TG profile of the fresh catalyst, a 2.4 wt.% mass-loss stage (from room temperature to 433 K) was owing to desorption of free solvent and water, and a 2.1 wt.% mass-increase stage (from 553 to 783 K) was attributed to the oxidation of metallic nickel. However, there were three mass-loss stages in the TG curve of the used catalyst: the first one (about 2.1 wt.%, from room temperature to 453 K) corresponded to desorption of free water and solvent, the second one (about 8.5 wt.%, from 473 to 758 K) and the third one (about 2.5 wt.%, above 833 K) to the oxidation of the organic species on the catalyst. Because the oxidation of the metallic nickel and the organic species occurred in the similar temperature range, the mass-increase stage due to the oxidation of metallic nickel in the used one was masked by the mass-loss stage of the oxidation of the organic species (as shown in Fig. 2(b)).

Fig. 2 also presents the oxidation DTA curves of the fresh catalyst and the used one. There was a remarkable exothermic

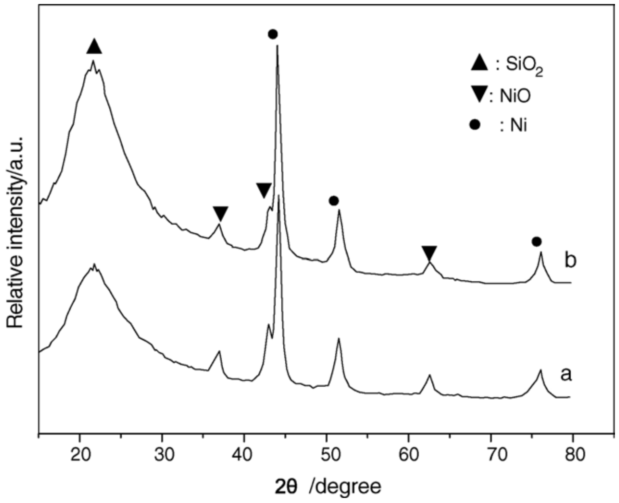

Fig. 1. XRD patterns of (a) fresh catalyst and (b) used catalyst.

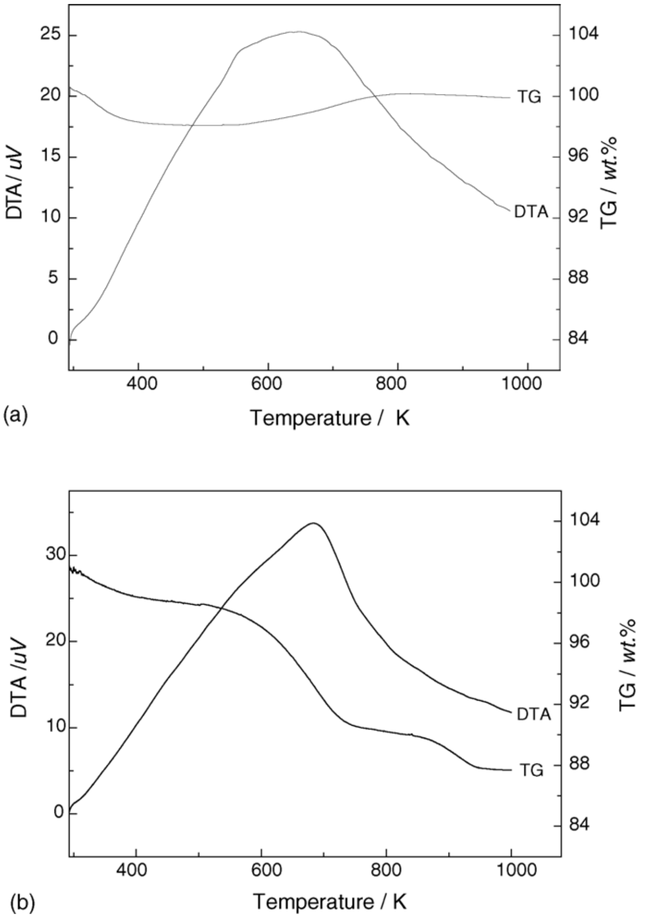

Fig. 2. TG and DTA profiles of (a) fresh catalyst and (b) used catalyst.

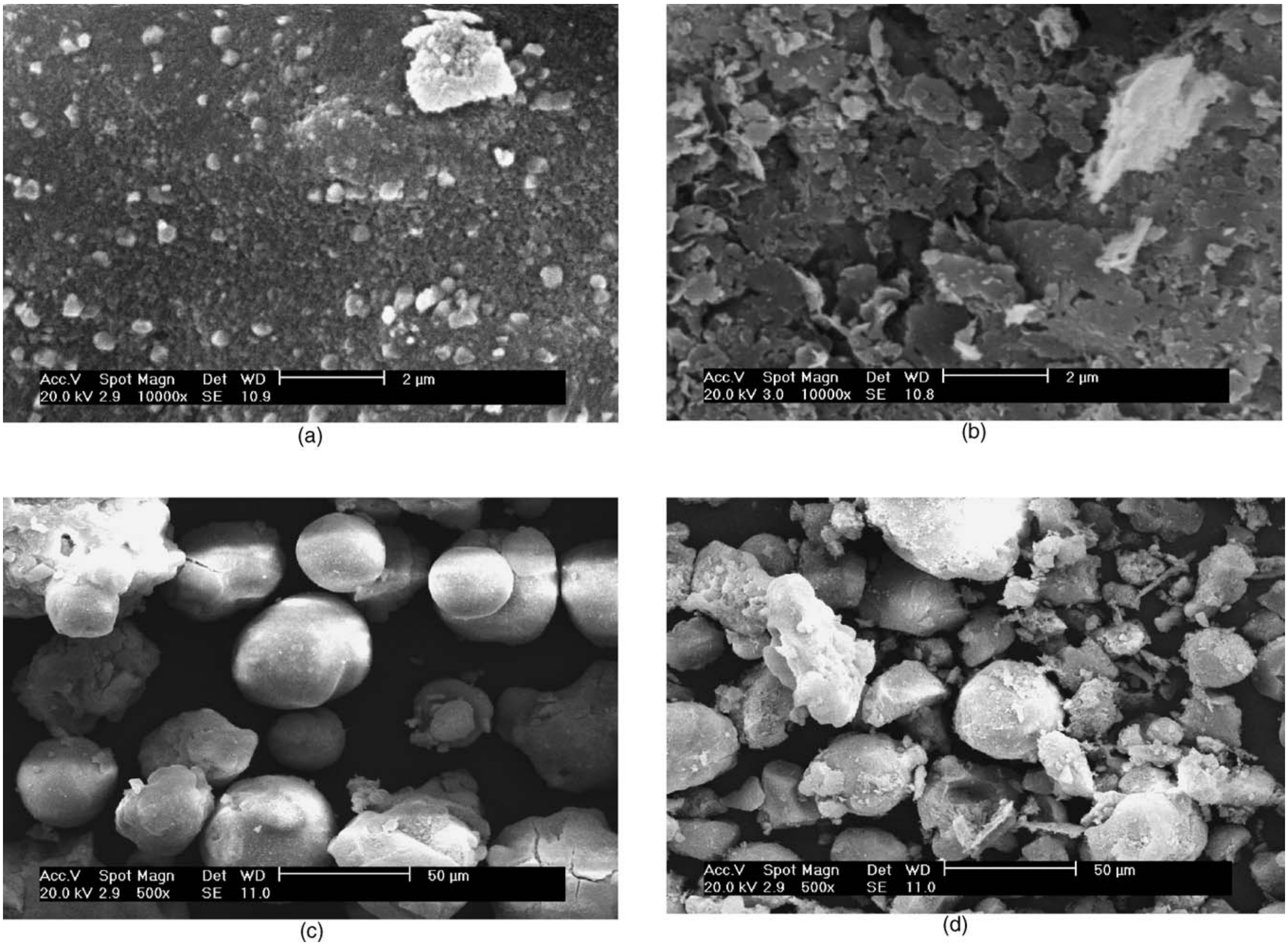

(a) (b) (c) (d)

Fig. 3. SEM micrographs of (a, c) fresh catalyst and (b, d) used catalyst.

peak in each DTA curve, about 646 K for the fresh catalyst and 684 K for the used one, the former corresponded to the oxidation of the metallic nickel and the later attributed to both of oxidation of the metal nickel and the organic species. Additionally, an inapparent peak of 956 K existed in DTA curve of the used catalyst, which was ascribed to the oxidation for more stable organic deposit. The results of DTA curves very coincided to those of TG curves.

3.2.3. *SEM results*

Fig. 3 shows the scanning electron micrographs of the fresh catalyst and the used one. For the used catalyst, there existed some sponge-like and faceted materials on its surface, which was related to the organic species. Besides, there were much smaller catalyst particles in the used catalyst than the fresh one. This phenomenon perhaps resulted from the mechanical stirring and the leaching of the catalyst as following mentioned. Table 3 lists ESEM-EDX analysis results of the two catalysts. Compared with the fresh catalyst, atomic ratios of Ni/Si and La/Si and K/Si on the surface of the used one decreased, while the C/Si atomic ratio increased. This fact further demonstrated that the surface of the used catalyst was covered with the organic species to some extent.

3.2.4. *BET and pore size distribution results*

Some textural properties of the fresh catalyst and the used one are summarized in Table 2. Compared with the fresh catalyst, the specific surface area and the pore volume of the used one decreased. Figs. 4 and 5 presents N_2 adsorption–desorption isotherm and pore size distribution, respectively. The isotherms of the two samples belonged to type-IV hysteresis loop [19], and the two samples showed a broad pore size distributions. In the used catalyst, however, the proportion of pore volume for smaller pores increased and that of larger pores decreased and the average pore radius became smaller.

It is well known that carbonaceous deposits occur in many catalytic reactions and they cover the catalyst surface, making the active sites inaccessible. Gallezot [15] once summarized the reasons for the catalyst deactivation in the liquid phase reac-

Table 3
Relative atomic ratio of elements on the surface of NLKS catalyst

Catalyst	Atomic ratio			
	Ni/Si	La/Si	K/Si	C/Si
Fresh sample	0.350	0.022	0.057	1.545
Used sample	0.275	0.016	0.030	2.365

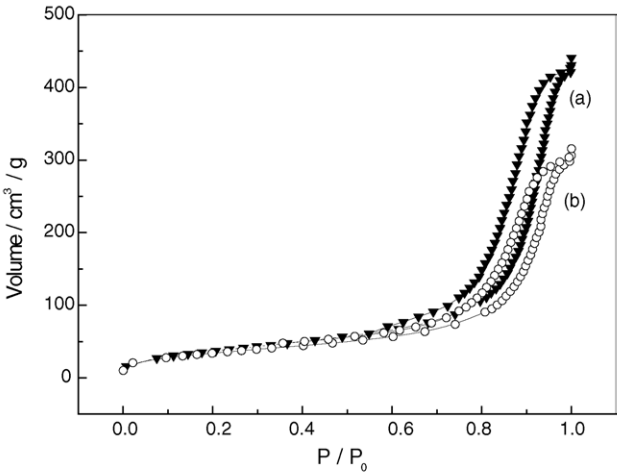

Fig. 4. N_2 adsorption–desorption isotherms of (a) fresh catalyst and (b) used catalyst.

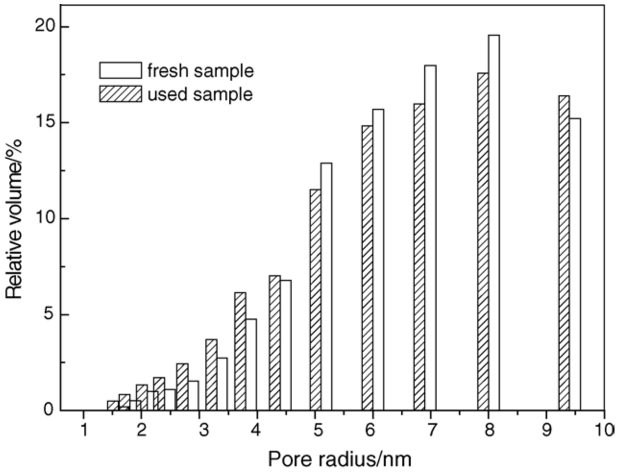

Fig. 5. Pore size distribution of fresh catalyst and used catalyst.

tions, and considered that reagents and oligomeric or polymeric by-products deposited on the surface of the catalyst were an important reason. However, formation of carbonaceous deposits on metal surfaces at room and slightly elevated temperature in catalytic hydrogenation is often neglected and scarcely studied [20]. Xiao and Hofmann [16] studied the deactivation of the Ni/SiO_2/Al_2O_3 in the hydrogenation of 3-hydroxypropanal. They found that the mesopore radius and the mesopore radius distribution of the fresh catalyst pellets were different from those of the deactivated catalyst. This fact indicated that some mesopores of the catalyst seem to be blocked by the formation of higher molecular by-products as they can cause the blockage of mesopores, but not of micropores.

Although there were no reports on the mechanism of hydrogenation of MDNB, it should be a complicated process deduced from the hydrogenation of nitrobenzene. Fig. 6 shows the mechanism of nitrobenzene hydrogenation [21]. There were some larger molecules produced in the hydrogenation process of nitrobenzene. Though these molecules could be converted to aniline eventually, they might adsorb on the surface of the catalyst easily and then block the pores; moreover, they might polymerize or/and condense to form more lager intermediates. Because there are two nitro-groups in a MDNB molecule, the hydrogenation process of MDNB should be more complicated and the intermediates should be much larger. These larger intermediates or those produced from polymerization would adsorb on the surface, block the pores (especially larger pores) and cover the metal nickel.

According to the results of N_2 adsorption–desorption, TG/DTA and SEM–EDX, it was considered that the surface coverage and the pore blockage with bulky molecular species was an important reason for the deactivation of NLKS catalyst.

3.2.5. AAS results

AAS analysis (showed in Table 2) indicated that Ni content of the fresh catalyst was 22.7 wt.%, and that of the used one was 20.3 wt.%, i.e., a part of nickel was lost during the reaction process.

The loss of the active component is also one of reasons for the catalyst deactivation and it usually results from the leaching of the active phase in liquid phase reactions. As far as metal catalyst is concerned, leaching of metal atoms depends on the reaction medium (pH, oxidation potential, chelating properties

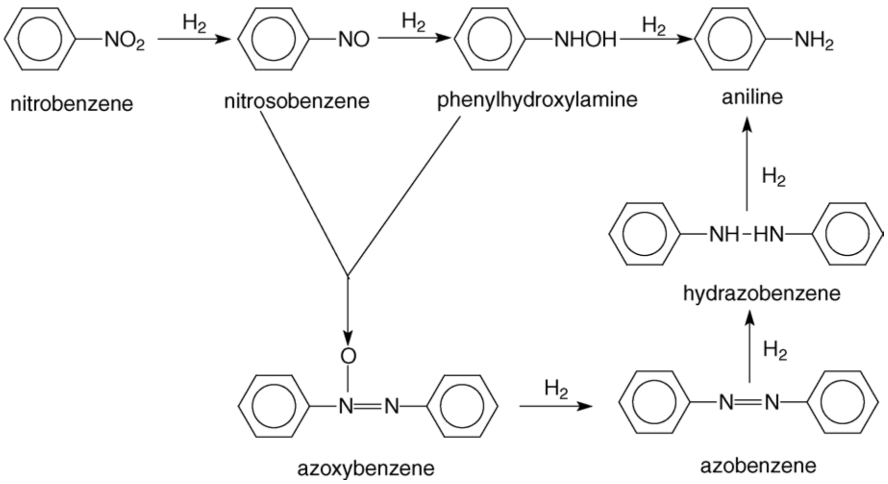

Fig. 6. Reaction scheme for nitrobenzene hydrogenation to aniline.

of molecules) and on bulk and surface metal properties. The metal-promoted Raney nickel catalysts underwent a drastic loss of activity in glucose hydrogenation after successive recycling because of the promoters leaching, especially iron and tin [22]. In the hydrogenolysis of aqueous solutions of sorbitol on CuO-ZnO catalysts to prepare C_4–C_6 polyols, zinc leaching was prevented by working under basic system [23]. In the present test, the concentration of nickel in the solution was about 13 ppm for the last recycle, which indicated the occurrence of nickel leaching. Because the products were the basic materials, pH value of the solution concerned was above 7.0, and so the leaching of Ni was very difficult. However, Silica belongs to acidic support and it can be leached in the basic medium. The leaching of silica would result in the loss of the supported metal nickel. In addition, an important parameter for long term performance is the mechanical stability of catalysts. In the present stirred bed reactor, the mechanical stress, resulting from the collisions of particles with each other and with reactor walls, could not only lead to mechanical abrasion of the active species from the support, but also make the catalyst broken up (as shown in Fig. 3(d)), all of which might also result in the loss of nickel.

4. Conclusion

Ni/La_2O_3-K_2O-SiO_2 catalyst showed better reactivity and stability in the hydrogenation of MDNB to MPD. With ethanol as solvent, under the conditions of 373 K, 3.0 MPa, catalyst/MDNB mass ratio of 3% and solvent/MDNB mass ratio of 2, the conversion of MDNB and selectivity of MPD were 99.9% and over 99.6%, respectively. There was a trend of catalyst deactivation along with recycles. The catalyst deactivation was mainly due to the surface coverage and the pore blockage with bulky molecular species. The loss of active component nickel was another reason. Growth of the nickel crystallites was rather slight and it did not influence the catalyst reactivity substantially.

References

[1] A.J. Bird, D.T. Thompson, Catalysis in Organic Syntheses, Academic Press, New York, 1980.
[2] H. Mizuta, T. Nishimura, M. Wada, T. Nagata, JP: 05 331 113 (1993).
[3] H. Mizuta, T. Nishimura, M. Wada, T. Nagata, JP: 6 009 511 (1994).
[4] K. Shimazu, Y. Tatrno, M. Magara, JP: 09132536 (1997).
[5] B. Pawelec, L. Daza, J.L.G. Fierro, J.A. Anderson, Appl. Catal. A 145 (1996) 307.
[6] P.A. Rautanen, J.R. Aittamaa, A.O.I. Krause, Chem. Eng. Sci. 56 (2001) 1247.
[7] D.J. Suh, T.J. Park, S.H. Lee, K.L. Kim, J. Non-Cryst. Solids 285 (2001) 309.
[8] T. Salmi, P. Mäki-Arvela, E. Toukoniitty, A.K. Neyestanaki, L.P. Tiainen, L.E. Lindfors, R. Sjöholm, E. Laine, Appl. Catal. A 196 (2000) 93.
[9] D. Jovanovic, R. Radovic, L. Mares, M. Stankovic, B. Markovic, Catal. Today 43 (1998) 21.
[10] S. Toppinen, T.K. Rantakylä, T. Salmi, J. Aittamaa, Catal. Today 38 (1997) 23.
[11] Y.X. Liu, Ph.D. Thesis, Tianjin University, China, 2003.
[12] Y.X. Liu, J.X. Chen, J.Y. Zhang, Chin. J. Catal. 24 (2003) 224.
[13] Y.X. Liu, J.X. Chen, J.Y. Zhang, Chin. J. Chem. Ind. Eng. 55 (2004) 37.
[14] G. Ertl, H. Knözinger, J. Weitkamp (Eds.), Handbook of Heterogeneous Catalysis, vol. 2, Wiley/VCH, New York/Weinheim, 1997.
[15] M. Besson, P. Gallezot, Catal. Today 81 (2003) 547.
[16] D.Zh. Xiao, H. Hofmann, Appl. Catal. A 155 (1997) 179.
[17] Y. Schuurman, B.F.M. Kuster, K. van der Wiele, G.B. Marin, Appl. Catal. A 89 (1992) 47.
[18] J.A.S. Bett, K. Kinoshita, K. Stonehart, J. Catal. 41 (1976) 124.
[19] G. Bergeret, P. Gallezot, in: J.M. Thomas, R.M. Lambert (Eds.), Characterisation of Catalysts, John Wiley & Sons Ltd., 1980.
[20] D.Yu. Murzin, E. Toukoniitty, J. Hájek, React. Kinet. Catal. Lett. 83 (2004) 205.
[21] V. Höller, D. Wegricht, I. Yuranov, L. Kiwi-Minsker, A. Renken, Chem. Eng. Technol. 23 (2000) 251.
[22] P. Gallezot, P.J. Cerino, B. Blanc, G. Flèche, P. Fuertesl, J. Catal. 146 (1994) 93.
[23] B. Blanc, A. Bourrel, P. Gallezot, T. Haas, P. Taylor, Green Chem. 2 (2000) 89.